

Measurement of the Average B Hadron Lifetime in Z^0 Decays Using Reconstructed Vertices

K. Abe,²⁹ I. Abt,¹⁴ C. J. Ahn,²⁶ T. Akagi,²⁷ N. J. Allen,⁴ W. W. Ash,^{27,*} D. Aston,²⁷ K. G. Baird,²⁴ C. Baltay,³³ H. R. Band,³² M. B. Barakat,³³ G. Baranko,¹⁰ O. Bardon,¹⁶ T. Barklow,²⁷ A. O. Bazarko,¹¹ R. Ben-David,³³ A. C. Benvenuti,² G. M. Bilei,²² D. Bisello,²¹ G. Blaylock,⁷ J. R. Bogart,²⁷ T. Bolton,¹¹ G. R. Bower,²⁷ J. E. Brau,²⁰ M. Breidenbach,²⁷ W. M. Bugg,²⁸ D. Burke,²⁷ T. H. Burnett,³¹ P. N. Burrows,¹⁶ W. Busza,¹⁶ A. Calcaterra,¹³ D. O. Caldwell,⁶ D. Calloway,²⁷ B. Camanzi,¹² M. Carpinelli,²³ R. Cassell,²⁷ R. Castaldi,^{23,†} A. Castro,²¹ M. Cavalli-Sforza,⁷ E. Church,³¹ H. O. Cohn,²⁸ J. A. Coller,³ V. Cook,³¹ R. Cotton,⁴ R. F. Cowan,¹⁶ D. G. Coyne,⁷ A. D'Oliveira,⁸ C. J. S. Damerell,²⁵ M. Daoudi,²⁷ R. De Sangro,¹³ P. De Simone,¹³ R. Dell'Orso,²³ M. Dima,⁹ P. Y. C. Du,²⁸ R. Dubois,²⁷ B. I. Eisenstein,¹⁴ R. Elia,²⁷ D. Falciari,²² C. Fan,¹⁰ M. J. Fero,¹⁶ R. Frey,²⁰ K. Furuno,²⁰ T. Gillman,²⁵ G. Gladding,¹⁴ S. Gonzalez,¹⁶ G. D. Hallewell,²⁷ E. L. Hart,²⁸ Y. Hasegawa,²⁹ S. Hedges,⁴ S. S. Hertzbach,¹⁷ M. D. Hildreth,²⁷ J. Huber,²⁰ M. E. Huffer,²⁷ E. W. Hughes,²⁷ H. Hwang,²⁰ Y. Iwasaki,²⁹ D. J. Jackson,²⁵ P. Jacques,²⁴ J. Jaros,²⁷ A. S. Johnson,³ J. R. Johnson,³² R. A. Johnson,⁸ T. Junk,²⁷ R. Kajikawa,¹⁹ M. Kalelkar,²⁴ H. J. Kang,²⁶ I. Karliner,¹⁴ H. Kawahara,²⁷ H. W. Kendall,¹⁶ Y. Kim,²⁶ M. E. King,²⁷ R. King,²⁷ R. R. Kofler,¹⁷ N. M. Krishna,¹⁰ R. S. Kroeger,¹⁸ J. F. Labs,²⁷ M. Langston,²⁰ A. Lath,¹⁶ J. A. Lauber,¹⁰ D. W. G. S. Leith,²⁷ M. X. Liu,³³ X. Liu,⁷ M. Loreti,²¹ A. Lu,⁶ H. L. Lynch,²⁷ J. Ma,³¹ G. Mancinelli,²² S. Manly,³³ G. Mantovani,²² T. W. Markiewicz,²⁷ T. Maruyama,²⁷ R. Massetti,²² H. Masuda,²⁷ E. Mazzucato,¹² A. K. McKemey,⁴ B. T. Meadows,⁸ R. Messner,²⁷ P. M. Mockett,³¹ K. C. Moffeit,²⁷ B. Mours,²⁷ G. Müller,²⁷ D. Muller,²⁷ T. Nagamine,²⁷ U. Nauenberg,¹⁰ H. Neal,²⁷ M. Nussbaum,⁸ Y. Ohnishi,¹⁹ L. S. Osborne,¹⁶ R. S. Panvini,³⁰ H. Park,²⁰ T. J. Pavel,²⁷ I. Peruzzi,^{13,‡} M. Piccolo,¹³ L. Piemontese,¹² E. Pieroni,²³ K. T. Pitts,²⁰ R. J. Plano,²⁴ R. Prepost,³² C. Y. Prescott,²⁷ G. D. Punkar,²⁷ J. Quigley,¹⁶ B. N. Ratcliff,²⁷ T. W. Reeves,³⁰ J. Reidy,¹⁸ P. E. Rensing,²⁷ L. S. Rochester,²⁷ J. E. Rothberg,³¹ P. C. Rowson,¹¹ J. J. Russell,²⁷ O. H. Saxton,²⁷ S. F. Schaffner,²⁷ T. Schalk,⁷ R. H. Schindler,²⁷ U. Schneekloth,¹⁶ B. A. Schumm,¹⁵ A. Seiden,⁷ S. Sen,³³ V. V. Serbo,³² M. H. Shaevitz,¹¹ J. T. Shank,³ G. Shapiro,¹⁵ S. L. Shapiro,²⁷ D. J. Sherden,²⁷ K. D. Shmakov,²⁸ C. Simopoulos,²⁷ N. B. Sinev,²⁰ S. R. Smith,²⁷ J. A. Snyder,³³ P. Stamer,²⁴ H. Steiner,¹⁵ R. Steiner,¹ M. G. Strauss,¹⁷ D. Su,²⁷ F. Suekane,²⁹ A. Sugiyama,¹⁹ S. Suzuki,¹⁹ M. Swartz,²⁷ A. Szumilo,³¹ T. Takahashi,²⁷ F. E. Taylor,¹⁶ E. Torrence,¹⁶ A. I. Trandafir,¹⁷ J. D. Turk,³³ T. Usher,²⁷ J. Va'vra,²⁷ C. Vannini,²³ E. Vella,²⁷ J. P. Venuti,³⁰ R. Verdier,¹⁶ P. G. Verdini,²³ S. R. Wagner,²⁷ A. P. Waite,²⁷ S. J. Watts,⁴ A. W. Weidemann,²⁸ E. R. Weiss,³¹ J. S. Whitaker,³ S. L. White,²⁸ F. J. Wickens,²⁵ D. A. Williams,⁷ D. C. Williams,¹⁶ S. H. Williams,²⁷ S. Willocq,³³ R. J. Wilson,⁹ W. J. Wisniewski,⁵ M. Woods,²⁷ G. B. Word,²⁴ J. Wyss,²¹ R. K. Yamamoto,¹⁶ J. M. Yamartino,¹⁶ X. Yang,²⁰ S. J. Yellin,⁶ C. C. Young,²⁷ H. Yuta,²⁹ G. Zapalac,³² R. W. Zdarko,²⁷ C. Zeitlin,²⁰ Z. Zhang,¹⁶ and J. Zhou²⁰

(SLD Collaboration)

¹Adelphi University, Garden City, New York 11530

²Instituto Nazionale di Fisica Nucleare (INFN) Sezione di Bologna, I-40126 Bologna, Italy

³Boston University, Boston, Massachusetts 02215

⁴Brunel University, Uxbridge, Middlesex UB8 3PH, United Kingdom

⁵California Institute of Technology, Pasadena, California 91125

⁶University of California at Santa Barbara, Santa Barbara, California 93106

⁷University of California at Santa Cruz, Santa Cruz, California 95064

⁸University of Cincinnati, Cincinnati, Ohio 45221

⁹Colorado State University, Fort Collins, Colorado 80523

¹⁰University of Colorado, Boulder, Colorado 80309

¹¹Columbia University, New York, New York 10027

¹²INFN Sezione di Ferrara and Università di Ferrara, I-44100 Ferrara, Italy

¹³INFN Laboratori Nazionali di Frascati, I-00044 Frascati, Italy

¹⁴University of Illinois, Urbana, Illinois 61801

¹⁵Lawrence Berkeley Laboratory, University of California, Berkeley, California 94720

¹⁶Massachusetts Institute of Technology, Cambridge, Massachusetts 02139

¹⁷University of Massachusetts, Amherst, Massachusetts 01003

¹⁸University of Mississippi, University, Mississippi 38677

¹⁹Nagoya University, Chikusa-ku, Nagoya 464, Japan

²⁰University of Oregon, Eugene, Oregon 97403

²¹INFN Sezione di Padova and Università di Padova, I-35100 Padova, Italy

²²INFN Sezione di Perugia and Università di Perugia, I-06100 Perugia, Italy

²³INFN Sezione di Pisa and Università di Pisa, I-56100 Pisa, Italy

²⁴Rutgers University, Piscataway, New Jersey 08855

²⁵Rutherford Appleton Laboratory, Chilton, Didcot, Oxon OX11 0QX, United Kingdom

²⁶Sogang University, Seoul, Korea

²⁷Stanford Linear Accelerator Center, Stanford University, Stanford, California 94309

²⁸University of Tennessee, Knoxville, Tennessee 37996

²⁹Tohoku University, Sendai 980, Japan

³⁰Vanderbilt University, Nashville, Tennessee 37235

³¹University of Washington, Seattle, Washington 98195

³²University of Wisconsin, Madison, Wisconsin 53706

³³Yale University, New Haven, Connecticut 06511

(Received 7 July 1995)

We report a measurement of the average B hadron lifetime using data collected with the SLD detector at the SLAC Linear Collider in 1993. An inclusive analysis selected three-dimensional vertices with B hadron lifetime information in a sample of 50×10^3 Z^0 decays. A lifetime of $1.564 \pm 0.030(\text{stat}) \pm 0.036(\text{syst})$ ps was extracted from the decay length distribution of these vertices using a binned maximum likelihood method.

PACS numbers: 14.65.Fy, 13.20.He, 13.30.-a, 13.38.Dg

Measurements of the B hadron lifetime τ_B are useful for exploring the physics of b quarks, particularly for determining the weak couplings of the b to lighter quarks. Precise measurements of the average value of τ_B remain interesting in view of the significant variation in the world average over the past few years (see Refs. [1–3]). Previous determinations of τ_B have relied on either hard lepton momentum cuts [4] or stringent vertex constraints to isolate B hadron decay vertices [5]. In the method presented here all decay modes are used with high efficiency.

In this Letter we present a measurement of τ_B based on inclusive three-dimensional reconstruction of secondary vertices in $Z^0 \rightarrow b\bar{b}$ events. The data for this analysis were collected at the SLAC Linear Collider (SLC) with the SLD experiment in 1993. The analysis used a topological technique to select vertices with lifetime information and relied on Monte Carlo (MC) modeling to extract τ_B using a maximum likelihood method. It yielded a precise measurement of τ_B , even with a relatively small data sample.

During the 1993 run SLD recorded 1.8 pb^{-1} of e^+e^- annihilation data at a center-of-mass energy of 91.26 ± 0.02 GeV. Charged particle tracking was provided by the central drift chamber (CDC) [6] and by the vertex detector (VXD) [7], with a combined impact parameter resolution in $r\phi(rz)$ parametrized as $\sigma = 11(38) \oplus 70/p\sqrt{\sin^3\theta} \mu\text{m}$, where p is expressed in GeV/ c . The liquid argon calorimeter [8] was used for triggering, thrust axis determination, and jet finding. The $\langle \text{rms} \rangle_{xyz}$ profile of the SLC beams was approximately $2.4 \times 0.8 \times 700 \mu\text{m}^3$ at the interaction point (IP). The x and y positions of the IP were continuously measured using reconstructed tracks from ~ 30 sequential hadronic Z^0 decays, giving $\sigma_{xy}^{\text{IP}} = 7 \pm 2 \mu\text{m}$ [9]. The z position was measured on an event-by-event basis using the median z position of tracks at their point-of-closest-approach to the IP in the x - y plane, with a resolution of $\sigma_z \approx 52 \mu\text{m}$ for $Z^0 \rightarrow b\bar{b}$ events [9].

A detailed simulation of the detector and physics processes was used in this analysis. Hadronic Z^0 decays were generated using JETSET 6.3 [10] adjusted to reproduce data from other e^+e^- experiments [11]. The fragmentation functions for b and c quarks followed the Peterson parametrization [12] with $\epsilon_b = 0.006$ and $\epsilon_c = 0.06$, respectively. A detailed description of the B hadron decay model may be found in Ref. [9]. Beam-related backgrounds and detector noise were simulated by overlaying random trigger events that occurred in close time proximity to recorded Z^0 decays. The detector response was simulated with GEANT 3.15 [13].

Hadronic Z^0 decays were selected by requiring at least 7 reconstructed tracks, total track energy greater than 18 GeV, and $|\cos\theta_{\text{thrust}}| < 0.71$ (thrust axis within CDC-VXD acceptance). A sample of 29 400 events was selected with a nonhadronic background estimated to be $< 0.1\%$.

A set of “quality” tracks for use in heavy quark tagging and vertexing was selected. Tracks measured in the CDC were required to have ≥ 40 hits, with the first hit at a radius $r < 39$ cm, a transverse momentum $p_{xy} > 0.4$ GeV/ c , a good fit quality ($\chi^2/N_{\text{DOF}} < 5$), and to extrapolate to the IP within 1 cm in x - y and 1.5 cm in z . Tracks were required to have at least one associated hit in the VXD, and a combined CDC-VXD fit with $\chi^2/N_{\text{DOF}} < 5$. Tracks with a 2D ($r\phi$) impact parameter $\delta > 3$ mm or with a 2D impact parameter error $\sigma_\delta > 250 \mu\text{m}$ were removed. Tracks from identified γ conversions, K^0 or Λ^0 decays were also removed. A discrepancy in the fraction of tracks passing quality track selection between data and MC was corrected by applying a momentum-dependent and angle-dependent correction of $\sim 6\%$ to the MC [9].

A sample of 4299 events with an enriched $Z^0 \rightarrow b\bar{b}$ content was tagged by choosing hadronic events having three or more quality tracks with normalized 2D impact parameter $\delta/\sigma_\delta > 3.0$. From the MC (with $\tau_B = 1.510$ ps), this algorithm was determined to be 60%

efficient at identifying $Z^0 \rightarrow b\bar{b}$ events and provided a 90% pure sample. The tag had a minimal effect on the measured lifetime due to a subsequent cut on flight distance, as will be discussed later.

Secondary vertex reconstruction and selection proceeded in three stages. In the first stage, quality tracks with $p > 1.0$ GeV/c were used to construct secondary vertices. Two-prong secondary vertices were constructed from all pairs of these tracks in an event hemisphere, defined with respect to the thrust axis, if they extrapolated to within 3 standard deviations of a common point in that hemisphere. If a track was shared between a pair of two-prong vertices, a three-prong vertex was also constructed. Four-prong vertices were constructed in a similar way. Tracks from three- and four-prong vertices were required to extrapolate to within 3 standard deviations of a common point. The vertex fit probability was required to be $>5\%$. To reduce the number of vertices containing tracks from the IP, the distance between each vertex and the IP was required to be greater than 1 mm, and at least one track in each vertex was required to have $\delta/\sigma_\delta > 2.5$. After these cuts, 97.8% of the 4299 tagged events contained at least one selected vertex.

On average, 6.5 vertices per hemisphere remained at this stage of the analysis. Figure 1(a) shows the number of vertices per event passing these selection criteria. The first column of Table I shows the composition of the vertices as determined from the MC; the first five categories carry lifetime information. A vertex was classified as “ b ” if all the tracks came from the weak decay of a B hadron, and as a “ b + cascade c ” if at least one track came from the weak decay of a B hadron and the rest from the weak de-

cay of a hadron containing a cascade c quark. The other categories were defined similarly.

Because of the loose vertexing criteria, most geometric vertices were reconstructed. However, tracks were allowed to contribute to more than one vertex. In the second stage of vertex selection, all possible sets (partitions) of independent vertices in each event hemisphere were found; i.e., each track was allowed to contribute to one vertex only. Events were rejected if the total number of partitions exceeded 1000. This removed 1.0% of tagged events. For each hemisphere, we selected the partition with maximum value of the product $M = \prod_{\text{all vertices}} P$, where P represents the vertex fit probability and the product includes all vertices in a given partition. The partition selection criterion was chosen to provide a high efficiency for finding vertices with lifetime information and low backgrounds. The true B hadron decay vertex was not necessarily reconstructed. Table I, column 2 shows the vertex composition after selection of the best partition, and Fig. 1(b) displays the distribution of the product M . To further reduce the background, particularly from vertices containing tracks from the IP, the angle between the vertex line of flight and the nearest jet axis was required to be less than 150 mrad, and each vertex track was required to have transverse momentum with respect to the vertex line-of-flight greater than 0.07 GeV/c. A sample of 5856 vertices (0.69 vertex/hemisphere on average) remained at this stage of the analysis. Figure 1(c) shows the distribution of the number of prongs per vertex.

In the third stage of vertex selection, one vertex was selected in each hemisphere in order to avoid multiple counting. For hemispheres containing more than one vertex, the vertex closest to the IP was selected to enhance contributions from b vertices over cascade c and other vertices. As a result, 60% of the hemispheres in the 4299 tagged events contained a selected vertex. Of the selected vertices, 92% contained a track associated with the weak decay of the B hadron. Figure 1(d) displays the total vertex momentum $|\sum_i \vec{p}_i|$ distribution at this stage. Table I, column 3 shows the vertex composition in the

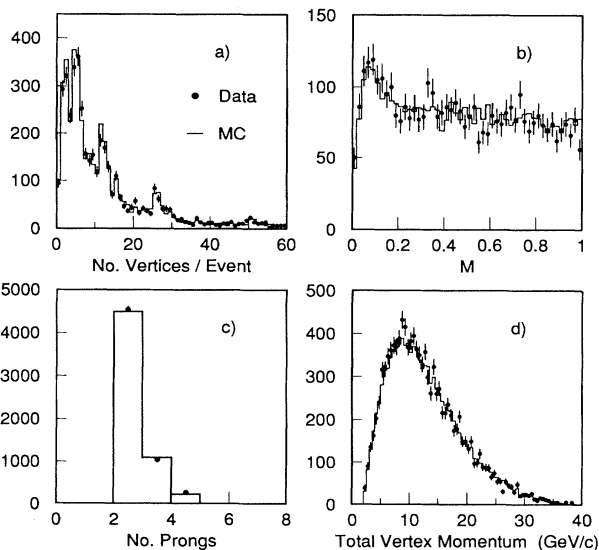


FIG. 1. Distribution of (a) number of vertices per event, (b) M , (c) number of prongs per vertex, and (d) total vertex momentum for data (points) and MC (histogram) with $\tau_B = 1.510$ ps, at different stages of vertex selection.

TABLE I. Vertex type in sample according to MC.

Vertex type	Stage 1 after initial vertex selection (%)	Stage 2 after partition selection (%)	Stage 3 final sample (%)
b	19	21	23
Cascade c	14	24	26
b + cascade c	48	35	37
b + other	9	5	3
Cascade c + other	5	6	3
Primary c	3	5	6
IP	0.5	1.3	0.4
Other	2	3	2
No. VTX/hemisph.	6.5	0.7	0.6

final sample. We have verified that data and MC matched closely at the various stages of vertex selection (see Fig. 1).

The B hadron lifetime was extracted from the decay length distribution (see Fig. 2), i.e., the distance between secondary vertices and the IP. A binned likelihood was computed for average lifetime values ranging between 0.7 and 2.3 ps; bins in the decay length distribution were combined to have a minimum of ten entries. The τ_B dependence in the MC was introduced by reweighting the decay length distribution of the B hadron component. The MC contained two sets of $Z^0 \rightarrow b\bar{b}$ decays. In the first set, B mesons (baryons), representing 91.1% (8.9%) of all B hadrons, were generated with an average lifetime of 1.55 ps (1.10 ps), and in the second set with 2.00 ps (1.42 ps). The average value of τ_B in the two MC sets was thus 1.510 and 1.948 ps, respectively. For the $\tau_B = 1.510$ ps MC sample, the B baryons represented 7.3% of all B hadrons after vertex selection. Using all MC samples, the maximum likelihood method yielded an average B hadron lifetime of $\tau_B = 1.564 \pm 0.030$ ps with a binned $\chi^2/N_{\text{DOF}} = 27.9/20$.

Systematic checks of the method and the detector modeling were performed. Independent samples of the $\tau_B = 1.510$ ps MC were used as data, yielding lifetimes in agreement with the generated lifetime. The lifetime was also extracted from the data using the $\tau_B = 1.510$ and 1.948 ps MC $Z^0 \rightarrow b\bar{b}$ samples separately, yielding values consistent with the reported result. In the two MC sets, the average values of the decay length distributions for each vertex type at the same reweighted τ_B were found to agree to within 1%. The measured lifetimes in different epochs of the run, i.e., under different run conditions, agreed within statistical errors as did measurements from four different azimuthal sections of the detector. We verified that the initial heavy quark tag had negligible effect by comparing the vertex composition and decay length

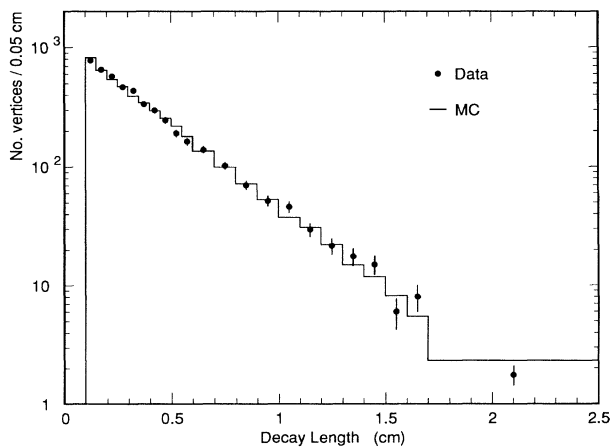


FIG. 2. Decay length distribution for vertices passing all selection criteria in data (points) and MC (histogram). The MC distribution corresponds to that with the best-fit lifetime.

distributions for tagged and untagged $Z^0 \rightarrow b\bar{b}$ events that passed all other cuts in the analysis. The 1 mm decay length cut reduced the backgrounds, especially from $Z^0 \rightarrow c\bar{c}$ events, and was found to reduce the sensitivity to the choice of tagging criteria. The tag was also investigated by considering only hemispheres opposite jets, which were tagged by requiring at least three tracks in the jet with $\delta/\sigma_\delta > 3.0$. This yielded an average lifetime of $\tau_B = 1.616 \pm 0.052$ ps, which was independent of the heavy quark tag and consistent with the reported result. The lifetime was insensitive to whether the closest or farthest vertex was chosen.

The systematic error due to detector modeling (see Table II) was dominated by the modeling of the reconstruction of quality tracks. This effect included both an overall normalization between data and MC after quality track selection, as well as a 0.3 track variation in quality track multiplicity between different run periods [9]. Track parameters were varied to reflect uncertainties in the radial and longitudinal alignment within the VXD and to account for the differences between data and MC in the tails of the IP position distribution along the z axis. The uncertainty due to the tails of the IP_{xy} position distribution was determined to be negligible.

The systematic errors due to the heavy quark physics modeling are also shown in Table II. The systematic errors due to b and c fragmentation were determined by varying ϵ_b and ϵ_c in the Peterson function used in our simulation [12] corresponding to $\langle x_E \rangle = 0.700 \pm 0.011$ for b fragmentation and $\langle x_E \rangle = 0.49 \pm 0.03$ for c fragmentation [14]. The b fragmentation systematic error also includes a contribution due to the uncertainty in the shape of the fragmentation function, which was estimated

TABLE II. Summary of systematic errors.

Error source	$\Delta\tau_B$ (ps)
Tracking efficiency	0.013
VXD alignment	0.005
b fragmentation	0.018
c fragmentation	0.005
Charm content of B decays	0.014
B baryon fraction	0.004
Charm hadron fraction	0.012
R_b	<0.001
R_c	0.002
B hadron decay multiplicity	0.009
D momentum spectrum in B decays	0.004
Charm hadron lifetime	0.004
Min. decay length in lifetime measurement	0.006
Decay length binning	0.007
Decay length cut in vertex selection	0.010
Vertex and partition limits	0.003
MC statistics	0.008
Total	0.036

by using the modified Bowler parametrization [15]. The sensitivity to the charm content of B hadron decays was estimated by taking into account the uncertainty in the B^0 and B^+ branching ratios [3]. The uncertainties were inflated by 100% to account for the fact that no data are available for B_s and B baryon branching ratios. The absolute fraction of B baryons in $Z^0 \rightarrow b\bar{b}$ events was varied by ± 0.05 . The absolute fractions of D^+ and charm baryons in $Z^0 \rightarrow c\bar{c}$ events were varied by ± 0.036 [16] and ± 0.03 , respectively. The multiplicity of tracks from B hadron decays was varied by ± 0.3 tracks to reflect the current uncertainty in this value [17]. The MC momentum spectra of D^+ and D^0 mesons from B hadron decays were adjusted to agree with recent CLEO data [18]. $R_b = \Gamma_{Z \rightarrow b\bar{b}} / \Gamma_{Z \rightarrow \text{hadrons}}$, $R_c = \Gamma_{Z \rightarrow c\bar{c}} / \Gamma_{Z \rightarrow \text{hadrons}}$, and the lifetimes of D^+ , D^0 , D_s , and Λ_c were varied by the uncertainties in their world averages [3].

The decay length bin size was varied from 0.25 to 2 mm and the minimum decay length used to extract the lifetime was varied from 1 to 3 mm. Samples passing different decay length cuts at the vertex reconstruction stage were fitted over the same range to assess the effect of this cut. The systematic error due to the cut on the maximum number of partitions was estimated to be negligible. This was accomplished by weighting the B hadron decay length distribution in the MC final sample to reproduce the distribution prior to the cut.

In conclusion, an inclusive vertexing technique was used to determine the average B hadron lifetime from an initial sample of 50×10^3 Z^0 decays. The measured lifetime was $1.564 \pm 0.030(\text{stat}) \pm 0.036(\text{syst})$ ps. This result confirms the higher lifetime values recently reported by other experiments [4,5].

We thank the personnel of the SLAC accelerator department and the technical staffs of our collaborating institutions for their outstanding efforts.

*Deceased.

[†]Also at the Università di Genova, I-16146 Genova, Italy.

[‡]Also at the Università di Perugia, I-06100 Perugia, Italy.

- [1] Particle Data Group, Phys. Rev. D **45**, S1 (1992), Part II.
- [2] W. Venus, in *Proceedings of the 16th Symposium on Lepton and Photon Interactions, Cornell University, 1993*, edited by P. Drell and D. Rubin (AIP, New York, 1993), p. 274.
- [3] Particle Data Group, Phys. Rev. D **50**, S1 (1994), Part I.
- [4] D. Buskulic *et al.*, Phys. Lett. B **295**, 174 (1992); P. D. Acton *et al.*, Z. Phys. C **60**, 217 (1993); O. Adriani *et al.*, Phys. Lett. B **317**, 474 (1993); F. Abe *et al.*, Phys. Rev. Lett. **71**, 3421 (1993).
- [5] P. Abreu *et al.*, Z. Phys. C **63**, 3 (1994).
- [6] M. Hildreth *et al.*, "Performance of the SLD Central Drift Chamber" (to be published).
- [7] C.J.S. Damerell *et al.*, in *Proceedings of the 26th International Conference on High Energy Physics, Dallas 1992* (World Scientific, New York, 1992), Vol. 2, p. 1862.
- [8] D. Axen *et al.*, Nucl. Instrum. Methods Phys. Res., Sect. A **238**, 472 (1993).
- [9] K. Abe *et al.*, Report No. SLAC-PUB-6569 (1994) (to be published).
- [10] T. Sjöstrand and M. Bengtsson, Comput. Phys. Commun. **43**, 367 (1987).
- [11] P. N. Burrows, Z. Phys. C **41**, 375 (1988); M. Z. Akrawy *et al.*, Z. Phys. C **47**, 505 (1990).
- [12] C. Peterson *et al.*, Phys. Rev. D **27**, 105 (1983).
- [13] GEANT 3.15 Program, CERN Applications Software Group, CERN Program Library (1993).
- [14] See, for example, R. Akers *et al.*, Z. Phys. C **60**, 601 (1993); D. Buskulic *et al.*, Z. Phys. C **62**, 1 (1994); D. Buskulic *et al.*, Z. Phys. C **62**, 179 (1994); P. Abreu *et al.*, Report No. CERN PPE/95-08, 1995.
- [15] M. G. Bowler, Z. Phys. C **11**, 169 (1981).
- [16] R. Akers *et al.*, Z. Phys. C **65**, 17 (1995).
- [17] H. Albrecht *et al.*, Z. Phys. C **54**, 13 (1992); R. Giles *et al.*, Phys. Rev. D **30**, 2279 (1984).
- [18] M. Thulasidas, Ph.D. thesis, Syracuse University, 1993.